EEG Mu (*μ*) Rhythm Spectra and Oscillatory Activity Differentiate Stuttering from Non-Stuttering Adults

Tim Saltuklaroglu, **Ashley W. Harkrider**[*], **David Thornton**, **David Jenson**, and **Tiffani Kittilstved**

University of Tennessee Health Science Center, Department of Audiology and Speech Pathology, 578 South Stadium Hall, Knoxville, TN, 37996, USA

Abstract

Stuttering is linked to sensorimotor deficits related to internal modeling mechanisms. This study compared spectral power and oscillatory activity of EEG mu (*μ*) rhythms between persons who stutter (PWS) and controls in listening and auditory discrimination tasks. EEG data were analyzed from passive listening in noise and accurate (same/different) discrimination of tones or syllables in quiet and noisy backgrounds. Independent component analysis identified left and/or right *μ* rhythms with characteristic alpha (*α*) and beta *(β)* peaks localized to premotor/motor regions in 23 of 27 people who stutter (PWS) and 24 of 27 controls. PWS produced *μ* spectra with reduced *β* amplitudes across conditions, suggesting reduced forward modeling capacity. Group time-frequency differences were associated with noisy conditions only. PWS showed increased *μ-β* desynchronization when listening to noise and early in discrimination events, suggesting evidence of heightened motor activity that might be related to forward modeling deficits. PWS also showed reduced *μ-α* synchronization in discrimination conditions, indicating reduced sensory gating. Together these findings indicate spectral and oscillatory analyses of *μ* rhythms are sensitive to stuttering. More specifically, these analyses can reveal stuttering-related sensorimotor processing differences in passive listening and auditory discrimination tasks which may be influenced by basal ganglia deficits.

Keywords

electroencephalography; internal modeling; mu *(μ)* rhythm; sensorimotor integration; stuttering

1. Introduction

Developmental stuttering is associated with widespread neural compromises in networks involved in timing (Alm, 2004;Howell, 2007;Chang and Zhu, 2013;Etchell et al., 2014) and sensorimotor integration (Max et al., 2004a;Loucks and De Nil, 2006;Loucks et al., 2007). Sensorimotor contributions to online speech monitoring and error detection are subserved by

[*]Tel.: +865-974-5019; fax: +865-974-5139. aharkrid@uthsc.edu.

internal modeling mechanisms. While speaking, premotor regions generate forward models via efference copy that contain predictions about the sensory consequences of forthcoming motor commands. These predictions are compared to speech targets and available reafference in sensory regions. Following comparison, sensory feedback is provided to the premotor regions that can be used to update motor commands and forward models (Shadmehr et al., 2010;Houde and Nagarajan, 2011;Keough and Jones, 2011;Houde and Chang, 2015). Within this mechanism, stuttering has been associated with weak forward models (Max et al., 2004a;Brown et al., 2005; Daliri and Max, 2015b;a) that may lead to a noisy comparison between prediction and reafference (Hickok et al., 2011;Tian and Poeppel, 2012), and a deficient feedback system (Neilson and Neilson, 1987;Corbera et al., 2005;Loucks and De Nil, 2006;Cai et al., 2012;Daliri and Max, 2015b). However, these hypotheses require further testing.

Support for sensorimotor deficits related to internal modeling can be found in structural and functional differences between people who stutter (PWS) and normally fluent counterparts. PWS exhibit reduced grey matter volume (Beal et al., 2007;Chang et al., 2008;Beal et al., 2013) and white matter connectivity in these regions (Sommer et al., 2002;Watkins et al., 2008;Chang and Zhu, 2013;Chang, 2014;Connally et al., 2014;Cieslak et al., 2015). However, discrepancies exist regarding how sensorimotor deficits manifest functionally. For example, though a meta-analysis showed stuttering to be associated with hyper-activation in left premotor regions (Brown et al., 2005), others have reported hypoactivation (Watkins et al., 2008;Chang et al., 2009;Kell et al., 2009;Loucks et al., 2011;Toyomura et al., 2011). Further, there is evidence from event-related potential studies of reduced speech induced suppression via internal modeling while producing speech in PWS relative to controls (Daliri and Max, 2015b;a). However, other studies have failed to show these differences (Beal et al., 2010). In many functional speech production studies, it is difficult to separate neural processes related to internal modeling from those directly involved in the execution of motor commands. Additionally, interpretation of neural speech production data in PWS is complicated by high variability in research designs and methods, the confounding influence of scanner noise in functional magnetic resonance imaging (fMRI) studies, speech rate, difficulties separating state from trait-based neural activity when speech is stuttered, and poor temporal resolution using fMRI measures (Wymbs et al., 2013;Belyk et al., 2015).

One means of overcoming some of these limitations is to examine internal modeling in speech perception. Categorical speech discrimination tasks, requiring attention and working memory, are known to recruit similar anterior dorsal sensorimotor networks (e.g., premotor and motor regions) necessary for speech production (Osnes et al., 2011;Grabski et al., 2013;Alho et al., 2014). In these tasks, cognitive load often is associated with dorsal stream activity, such that discrimination in noisy conditions typically elicits greater sensorimotor activity than in quiet conditions (Binder et al., 2004;Callan et al., 2010;Alho et al., 2012;Bowers et al., 2013). Internal modeling mechanisms may play dynamic roles across the time course of accurate discrimination. Prior to stimulus presentation, forward models can provide predictions about forthcoming stimuli that help constrain the auditory analysis as the stimuli are perceived (Callan et al., 2010;Arnal, 2012;Arnal and Giraud, 2012;Pecenka et al., 2013;Callan et al., 2014;Mathias et al., 2015). Following stimulus offset, stimuli are preserved in working memory (Hickok et al., 2003;Burton, 2009;Sato et

al., 2009;Baddeley, 2010), which may be aided by updating internal models following auditory stimulation (Jenson et al., 2014).

Ample evidence also exists for recruitment of anterior dorsal regions during non-speech discrimination (Joanisse and Gati, 2003;Zaehle et al., 2008;Scott et al., 2009). Tone stimuli typically are associated with stronger right hemisphere activity (Pugh et al., 1996;Celsis et al., 1999;Zatorre et al., 1999;Liebenthal et al., 2013). However, there is evidence that in more complex discrimination tasks, speech and tone stimuli recruit similar sensorimotor networks (Fiez et al., 1996;Poldrack et al., 2001;Joanisse and Gati, 2003;LoCasto et al., 2004;Burton and Small, 2006), a finding that has been attributed to attempts to internally simulate tone stimuli (Hickok and Poeppel, 2004;Burton, 2009). Thus, examining sensorimotor activity across the time course of auditory discrimination likely will reveal important information about the changing dynamics of dorsal stream activity in both normal and stuttering populations during the processing of speech and non-speech stimuli.

Auditory perception studies in PWS have produced important findings. These include evidence that PWS rely more heavily on the right hemisphere for speech processing (Weber-Fox et al., 2004;Liotti et al., 2010; Robb et al., 2013;Halag-Milo et al., 2016) and exhibit differences in left hemisphere activity patterns for complex speech processing but not for simple tone processing (Biermann-Ruben et al., 2005;Corbera et al., 2005). ERP responses to speech stimuli in adults (Beal et al., 2010) and children (Beal et al., 2011;Jansson-Verkasalo et al., 2014) who stutter also suggest evidence of auditory-motor integration deficits. There is also behavioral evidence to suggest that PWS perform more poorly than controls in speech (Neef et al., 2012;Lu et al., 2016) and non-speech (Hampton and Weber-Fox, 2008) perception tasks and perceptual difficulties might be related to functional connectivity across speech motor regions (Lu et al., 2016) and auditory processing (Hampton and Weber-Fox, 2008). However, it is still not known how sensorimotor contributions for speech and tone discrimination differ between PWS and controls over the time course of events.

Examination of mu (μ) rhythms (Pineda, 2005;Hari, 2006) offers a novel means of investigating sensorimotor differences associated with stuttering. Using independent component analysis (ICA), μ rhythms easily can be identified based on their two peaks; one within alpha (α; 8–14 Hz) and one within beta (β; 15–25 Hz) frequencies (Niedermeyer and da Silva, 2005;Pineda, 2005;Hari, 2006). Though they can be observed in various regions of the cortex (Schnitzler et al., 2000;Hauswald et al., 2013;Kodama et al., 2016), the primary sources of μ rhythms lie within anterior regions of the dorsal stream (e.g., premotor and primary motor cortices). Within sensorimotor μ rhythms, activity in the β band is thought to encode motor information (Pfurtscheller, 1981;Toro et al., 1994;Seeber et al., 2014), and activity within the α band is thought to encode somatosensory and auditory feedback (Cheyne et al., 2003;Gaetz and Cheyne, 2006;Tamura et al., 2012;Sebastiani et al., 2014;Peled-Avron et al., 2016). Thus, if stuttering is associated with reduced capacity for generating forward models in motor regions, μ spectral differences, particularly in β frequencies, might be expected when comparing PWS to non-stuttering groups.

Suppression of μ rhythm power has been used to index sensorimotor activity associated with many visual (Urgen et al., 2013;Frenkel-Toledo et al., 2014;Ruther et al., 2014) and auditory (Pineda et al., 2013;Tsuchida et al., 2015) perception tasks, including speech (Crawcour et al., 2009;Cuellar et al., 2012;Pineda et al., 2013). In these studies, only α frequencies were considered, possibly because activity in α and β bands often is correlated highly (Carlqvist et al., 2005;de Lange et al., 2008). However, there is evidence to suggest that α and β oscillatory activity provide distinct, though cooperating, contributions to sensorimotor control and processing (Brinkman et al., 2014). In addition to indexing motor activity, β fluctuations index general attention (Engel and Fries, 2010), top-down predictive coding in perceptual decision-making (Donner et al., 2009;Arnal and Giraud, 2012;Cheyne, 2013), and maintenance of a stimulus in working memory (Lewis et al., 2016). α waves are ubiquitous across the brain and suppression of their power is implicated in many cognitive and working memory tasks (Klimesch, 2012;Gao et al., 2015;Pandey et al., 2016). Conversely, α power enhancement is considered a marker of inhibitory activity associated with disregarding irrelevant stimuli or redistributing neural activity to another cortical region (Jensen and Mazaheri, 2010); processes which also may be disrupted in PWS (Civier et al., 2010;Kikuchi et al., 2011;Chang and Zhu, 2013;Civier et al., 2013). Thus, within unified μ rhythms, examining activity in α and β channels simultaneously across time should provide important indices of sensorimotor contributions to various tasks.

Time-frequency analysis exploits the temporal resolution of EEG, measuring fluctuations in oscillatory power across specific events, to reveal changes in cortical processing across time. Oscillatory fluctuations typically are measured as event-related synchronization (ERS), suggesting neural inhibition and event-related desynchronization (ERD), suggesting neural activation. Two recent studies (Bowers et al., 2013;Jenson et al., 2014) applied ICA to identify μ components in accurate auditory (syllable and tone sweep) discriminations and then, applied time-frequency analyses to map the temporal dynamics of sensorimotor activity over time via fluctuation in α and β channels. The patterns of changing oscillatory activity, beginning before stimulus onset, were interpreted in light of the dynamic roles dorsal stream processing may play in auditory discrimination. Both studies revealed μ-β ERD prior to stimulus onset, suggestive of a top-down predictive role. Further, the Jenson et al. (2014) study found significant μ-α ERS prior to and during stimulus onset, which was stronger when stimuli were discriminated in noisy backgrounds, suggesting that inhibitory processes also may facilitate sensory predictions in these tasks. Following stimulus offset, μ-α and μ-β ERD were observed. This pattern also is found in speech production and suggests stimuli are held in working memory and possibly covertly replayed prior to a response (Jenson et al., 2014;Jenson et al., 2015).

Thus, after identifying left and right μ components in PWS and matched non-stuttering controls in classic speech and tone discrimination tasks (similar to those used in Bowers et al., 2013 and Jenson et al., 2014; 2015), the aims of the current study are twofold. The first is to compare the spectral power of μ rhythms between the groups. It is hypothesized that stuttering will be characterized by weaker μ rhythms, especially in the β band, which is associated with motor function and forward modeling. The second aim is to make comparisons of α and β oscillatory activity across the time course of each condition and between the two groups. Event-related differences in μ-α and μ-β oscillatory activity across

time are likely to reveal sensorimotor differences related to speech and tone processing in quiet and noisy conditions for stuttering and non-stuttering populations. Together, the findings will test hypotheses about the nature of forward modeling and sensory feedback deficits in stuttering.

2. Materials and Methods

2.1. Subjects

People Who Stutter: Twenty-seven native English speakers with developmental stuttering were initially recruited. Subjects (8 females, 19 males) had a mean age of 26.9 years (range 17–52) and no history of other cognitive, communicative, or attentional disorders. Three of the 27 PWS were left-handed. Table 1 provides a summary of the PWS participants' age, sex, handedness using the Edinburgh Handedness Inventory (Oldfield, 1971), and stuttering severity according to the Stuttering Severity Instrument (SSI-4) (Riley, 2009). The table also shows which participants yielded usable left or right μ components.

Control subjects who are native English speakers, do not stutter and had no history of other cognitive, communicative, or attentional disorders were recruited such that they were age (within 3 years), gender, and handedness matched to PWS who yielded left or right μ components. It was necessary to recruit a total of twenty-seven controls (8 females, 19 males with an average age of 27.5 years) to provide matches for all PWS who contributed usable left or right μ components.

The Institutional Review Board (IRB) for the University of Tennessee approved this work as a study with minimal risks to human subjects (IRB# 09-00464-XP), and all subjects provided informed consent prior to participation. Syllable stimuli (/ba/ and /da/) were generated with AT&T naturally speaking text-to-speech software, using synthetic analogs of a male speaker (Bowers et al., 2013;Bowers et al., 2014;Jenson et al., 2014;Jenson et al., 2015). Stimuli then were low pass filtered at 5 kHz and normalized for RMS (root-mean-square) amplitude. Syllable pairs were created such that half of the stimuli pairs were identical (e.g./ba/-/ba/) and half were different (e.g./da/-/ba/). Each syllable was 200 ms in duration and paired syllables were separated by 200 ms (inter-stimulus interval). Thus, the total duration of stimuli presentation was 600 ms from onset of the first syllable to offset of the second syllable.

To control for task difficulty and stimulus length, tone sweeps were constructed to match the structure of the syllables, similar to Bowers et al. (2013). Tone-sweep stimuli were generated with an 80 ms modulated tone onset and a 120 ms steady state 1000 Hz sine wave. Like the speech stimuli, tone sweeps were low-pass filtered at 5 kHz and normalized for RMS amplitude. Tone pairs differed only in whether the pitch onset was lower (750 Hz) or higher (1250 Hz) than the 1000-Hz steady state tone. Thus, the duration and structure of the tone stimuli were constructed to mimic the rising (/ba/) and falling (/da/) F2 transitions in the syllables (Joanisse and Gati, 2003). Tone pairs were created such that half of the stimuli pairs were identical and half were different. Similar to the speech stimuli, each tone sweep was 200 ms in duration and paired tones were separated by 200 ms (interstimulus interval).

Thus, the total duration of stimuli presentation was 600 ms from onset of the first tone sweep to offset of the second.

All stimuli were presented at 70 dB SPL. Two of the active discrimination conditions required subjects to discriminate tone pairs or syllable pairs embedded in white noise with a signal-to-noise ratio (SNR) of +4 dB. These conditions were included, as previous studies have reported that this SNR produces increased dorsal stream activity while allowing participants to accurately discriminate between the syllables (Binder et al., 2004;Osnes et al., 2011;Bowers et al., 2013;Bowers et al., 2014).

2.3. Design

The experiment consisted of a 5 condition × 2 group mixed design. The five conditions were:

1.   Passive listening to white noise (PN)

2.   Discrimination of tone pairs in quiet (TQ)

3.   Discrimination of tone pairs in noise (TN)

4.   Discrimination of syllable pairs in quiet (SQ)

5.   Discrimination of syllable pairs in noise (SN)

Condition 1 was a passive listening task and conditions 2 – 5 were active discrimination tasks, each requiring categorical same-different judgments of the stimulus pairs within the condition. In order to control for a discrimination response bias (Venezia et al., 2012), an equal number of different and identical syllable pairs were used in each discrimination condition. The PN condition required no discrimination, but was used as a reference task for the four other conditions. A button press response also was used in the PN condition for two reasons: (1) to control for anticipatory β suppression which has been previously reported in tasks requiring a button press response (Makeig et al., 2004;Graimann and Pfurtscheller, 2006;Hari, 2006) and (2) requiring a button press response in a condition with no active discrimination ensured that the subjects were attending to and engaged in the task. To help ensure that anticipatory β suppression related to the button press had minimal influence on neural activity, the button press was required 3000 ms following stimulus onset and was not included in the epoch that ended 2000 ms following onset (Alegre et al., 2003). In addition, a sufficiently long inter-trial interval was used to ensure that beta rebound, which can occur up 1250 ms post button press (Jurkiewicz et al., 2006), did not contaminate baselines of subsequent trials. Figure 1 depicts the time-line for trials in all conditions, showing the control (PN) and discrimination (TQ, TN, SQ, SN) conditions. Included is the 3500 ms inter-trial intervals, from which 1000 ms baselines for each trial were selected at the end of the interval.

2.4. Procedure

Procedures were adapted from previous studies (Bowers et al., 2014;Jenson et al., 2014;Jenson et al., 2015). The experiment was conducted in an electrically and magnetically shielded, double-walled, sound treated booth. Participants were seated in a comfortable chair

with their heads and necks supported. Stimuli were presented and button press responses were recorded by a PC computer running Compumedics NeuroScan Stim 2, version 4.3.3. The response cue for all perception conditions was a 100 ms, 1000 Hz tone presented following the end of the trial epoch (i.e., 3000 ms post stimulus onset, see figure 1). In the PN condition, subjects were instructed to sit quietly, listen to the stimulus (i.e., white noise), and press the button when they heard the response cue. In the quiet and noisy discrimination conditions, subjects were instructed to press one of two buttons after hearing the response cue depending on whether the tone pairs or syllable pairs were judged to be the same or different. Handedness of button press response was counterbalanced across all subjects and conditions. Discrimination accuracy was determined as percentage of trials correctly discriminated, and subjects who did not discriminate at a level significantly above chance were excluded from the analysis. Each of the five conditions were comprised of 2 blocks of 40 trials, yielding 10 blocks total (5 conditions × 2 blocks). Order of presentation of blocks was randomized for each subject.

2.5. EEG Acquisition

Whole head EEG data were acquired from 68 channels. These channels included two electromyography electrodes that were placed at midline on the upper and lower lips and two electrocardiogram electrodes placed on the neck over the left and right common carotid arteries. Data were recorded with an unlinked, sintered NeuroScan Quik Cap, based on the extended international standard 10–20 system (Jasper, 1958;Towle et al., 1993). All recording channels were referenced to the linked mastoid channels (M1, M2) and the ground was placed between Fz and Fpz. The electro-oculogram was recorded by means of two electrode pairs placed above and below the orbit of the left eye (VEOL, VEOU) and on the medial and lateral canthi of the left eye (HEOL, HEOR) to monitor vertical and horizontal eye movement.

EEG data were recorded using Compumedics NeuroScan Scan 4.3.3 software in tandem with the Synamps 2 system. EEG data were band pass filtered (0.15 – 100 Hz) and digitized with a 24-bit analog to digital converter with a sampling rate of 500 Hz. Data collection was time locked to stimulus onset. Thus, time zero was defined as stimulus onset in all discrimination conditions.

2.6. EEG Data Processing

Data processing and analysis were performed with EEGLAB 13 (Brunner et al., 2013), an open source MATLAB toolbox. Processing occurred at the individual level and data were analyzed at both the individual and group level. The following steps were performed at each stage:

1. Individual processing/analysis:

    a. Preprocessing of 10 raw EEG files for each participant (5 conditions × 2 blocks).

    b. Independent Component Analysis (ICA) of preprocessed files across conditions for each participant.

> **c.** Localization of dipoles for each independent component.

2. Group analysis:

> **a.** The STUDY module within EEGLAB 13 was used to perform analysis on neural components.
>
> **b.** Components common across participants were clustered by means of Principal Component Analysis (PCA).
>
> **c.** Left and right μ clusters were identified and components were checked to ensure that they met inclusion criteria.
>
> **d.** Mean left and right μ cluster sources were localized by equivalent current dipole (ECD) and verified by current source density (CSD) methods.
>
> **e.** Changes in spectral power over time in μ clusters were identified by measuring event related spectral perturbations (ERSP).

2.7. Data preprocessing

Raw EEG data files from both blocks of each condition were appended to create one dataset per condition per participant consisting of 80 trials, and then resampled to 256 Hz to reduce the computational requirements of further processing steps. Trial epochs of 5000 ms (ranging from −3000 to +2000 ms around time zero, which corresponded with stimulus onset) were extracted from the continuous EEG data. The data then were filtered from 3 – 34 Hz, which allowed for clear visualization of α and β bands while filtering muscle artifact from surrounding frequency bands. All EEG channels were referenced to the mastoids (M1, M2) to remove common mode noise. Trials were visually inspected and all epochs containing gross artifact (in excess of 200 μV) were removed. To help control for attention, trials were rejected and excluded from further analysis if the participant performed the discrimination incorrectly or if the response latency exceeded 2000 ms, which would be considered an unusually late response. A minimum of 40 usable trials per condition per participant was required in order to ensure a successful ICA decomposition.

2.8. Independent Component Analysis (ICA)

Following data preprocessing and prior to ICA decomposition, data files for each participant were concatenated to yield a single set of ICA weights common to all conditions. This allowed for comparison of activity across conditions within spatially fixed components. The data matrix was decorrelated through the use of an extended Infomax algorithm (Lee et al., 1999). Subsequent ICA training was accomplished with the "extended runica" algorithm in EEGLAB 13 with an initial learning rate of 0.001 and the stopping weight set to 10^{-7}. ICA decomposition yielded 66 ICs for each participant, corresponding to the number of recording electrodes (68 data channels with 2 reference channels; M1, M2). These included components from both neural and non-neural (e.g., muscular, artifactual) sources, demonstrating how ICA is an excellent tool for unmixing volume conducted EEG signals (Bell and Sejnowski, 1995; Makeig et al., 1996; Makeig et al., 1997). Scalp maps for each

component were generated by projecting the inverse weight matrix (W-1) back onto the original spatial channel configuration.

After ICA decomposition, an equivalent current dipole model (ECD) was computed for each IC by using the Brain Electrical Source Analysis (BESA) spherical model in the DIPFIT toolbox, an open source MATLAB plugin available at sccn.ucsd.edu/eeglab/dipfit.html (Oostenveld and Oostendorp, 2002). Electrode coordinates conforming to the standard 10–20 configuration were warped to the head model. Automated coarse-fitting to the BESA head model revealed a single dipole for every IC generated by all paticipants. Hence, all cortical and non-cortical sources of EEG activity could be identified. Dipole source localization involved a back projection of the signal to a potential source that could have generated the signal, followed by computing the best forward model from that hypothesized source that accounts for the highest proportion of the scalp recorded signal (Delorme et al., 2012). The residual variance (RV) is the mismatch between the original scalp recorded signal and this forward projection of the ECD model. The RV can be interpreted as a goodness of fit measure for the ECD model.

2.9. STUDY (Group level) analyses

Group level analyses were performed in the EEGLAB STUDY module using only neural components from the original ICA analyses. The STUDY module allows for the comparison of ICA data across participants and conditions. Principal component analysis (PCA) initially was used to cluster the pool of 2942 neural components with less than 20% RV from all participants. PCA clustering was conducted based on similarities in scalp maps, spectra, and dipole locations across components. A total of 40 clusters of neural activity from contributing participants were identified, including clusters composed mainly of left and right μ components. All components within identified μ clusters were checked against the a priori inclusion criteria of being localized to premotor (BA 6), primary motor (BA 4) or primary somatosensory (BA 1,2,3) regions, having a characteristic spectral shape including α and β peaks, and a RV threshold of <20%, similar to Jenson et al. (2014) and Bowers et al. (2013). Those that did not meet the criteria were removed from the cluster and not considered in the analysis. Neighboring clusters also were checked for components with μ characteristics to ensure that PCA had not misplaced any components. Left or right μ components meeting inclusion criteria that PCA had misplaced were reassigned to the appropriate μ cluster. Because of the manner in which ICA decomposes EEG data, it was possible that some participants did not contribute components that met inclusion criteria for the μ clusters. In addition, due to the fact that 64 neural recording channels produced the same number of ICs (Makeig et al., 2004), it was possible for participants to contribute multiple components to each cluster. Once μ clusters had been established, all components within the clusters were checked by a second rater to ensure agreement on cluster membership.

2.10. Source localization

Source localization for ECD clusters identified in the STUDY module is the mean of the Talairach coordinates (x, y, z) for each of the contributing dipole models (identified by the DIPFIT module). Verification of ECD localization was conducted using another method of

source localization known as standardized low-resolution brain electromagnetic tomography (sLORETA). sLORETA addresses the inverse problem by using current source density (CSD) from scalp recorded electrical signals to estimate source location (Pascual-Marqui, 2002). Solutions are based on the Talairach cortical probability brain atlas, digitized at the Montreal Neurological Institute (MNI). Electrode locations are co-registered between both spherical models (BESA) and realistic head geometry (Towle et al., 1993). The 3-D brain space was divided into 6,239 voxels, yielding a spatial resolution of 5 mm. The inverse weight projections from the original EEG channels for each component contributing to the μ clusters were exported to sLORETA. Cross-spectra were computed and mapped to the Talairach atlas and cross-registered with MNI coordinates, resulting in CSD estimates for each contributing component. The analysis of statistical significance of CSD estimates across participants was performed in the sLORETA software package. The analysis was non-parametric, based on the estimation (via randomization) of the probability distribution of the t-statistic expected under the null hypothesis (Pascual-Marqui, 2002). This method corrects for multiple comparisons across all voxels and frequencies (3–34 Hz). Voxels that were significant at $p < 0.001$ were considered active across participants. Group level source localizations are based on the CSD source estimates computed via sLORETA. ECD localizations also are reported, as they serve to demonstrate the inter-subject variability present in the data.

2.11. Time-frequency analyses

Event-related spectral perturbation (ERSP) analyses were used to measure fluctuations in spectral power (in normalized decibel units) across time in the frequency bands of interest (3 – 34 Hz). Time-frequency transformations were computed using a Morlet wavelet rising linearly from 3 cycles at 3 Hz to 25.6 cycles at 34 Hz. Trials were referenced to a pre-stimulus baseline selected from the last second of the 3500 ms inter-trial interval. A surrogate distribution was generated from 200 randomly sampled latency windows from this silent baseline (Makeig et al., 2004). Individual ERSP changes across time were calculated with a bootstrap resampling method ($p < 0.05$ uncorrected). Single trial data for all experimental conditions for frequencies between 4 and 30 Hz and ranging from −500 to 1500 ms were entered into the time-frequency analysis. This frequency window adequately captured α and β oscillatory activity, while the time window captured activity before, during, and after stimulus presentation.

2.12. Statistical analyses

For both spectral and time-frequency data, pairwise permutation statistics (2000 permutations) were used for comparisons across the 5 conditions (PN, TQ, TN, SQ, SN), in addition to quiet (TQ and SQ) versus noisy (TN and SN) discrimination contrasts and tone (TQ and TN) versus speech (SQ and SN) discriminations contrasts. Unpaired permutation statistics were used to compare between the two groups. Type 1 error was controlled by a cluster-based nonparametric statistical correction for multiple comparisons (Maris and Oostenveld, 2007). To examine a possible relationship between stuttering severity and β power, a Pearson correlation analysis was performed between power at the μ-β peak maxima (extracted from spectra) in the PN condition and total raw SSI scores in PWS for both left and right μ components. Spectra were undifferentiated by condition. However, spectra from

the PN task were selected for the correlation analysis, as it was the condition with fewest time frequency changes across the trial epoch. Total raw SSI scores were selected, as they are robust measures of severity that are influenced by stuttering frequency, duration, and ancillary behaviors. For participants who contributed more than one component to a cluster, the average power for β peak maxima was used in the correlation.

3. Results

3.1. Discrimination accuracy

Figure 2 shows discrimination accuracy by group. A mixed ANOVA performed on root-arcsine transformed proportions examined the effects of stimulus type (speech versus tone), background (quiet versus noisy) and group (controls versus PWS) on accuracy level. Significant effects were observed for stimulus type [$F(1,44)= 47.10$, $p< 0.001$], group [$F(1,44)=10.36$, $p= 0.002$], and the stimulus type $\times$ group interaction [$F(1,44)= 7.68$, $p= 0.008$], demonstrating that tone conditions were discriminated less accurately in PWS only. Bonferroni corrected post hoc unpaired t-tests showed that PWS were significantly less accurate than controls in the TQ condition only [$t(44) =3.65$, $p= 0.001$]. No significant effects or interactions for background were found. The high accuracy levels overall suggest participants attended to the tasks and produced sufficient accurate trials from each condition for EEG analysis.

3.2. μ cluster characteristics

For the PWS that contributed to μ clusters (below), the average number of usable (i.e., accurate and clean) trials for each condition was: PN = 67.0 (SD = 10.3); TQ = 57.0 (SD = 9.8); TN = 58.5 (SD = 10.4); SQ = 63.3 (SD = 10.1); SN = 59.1 (SD = 12.6). For the control participants that contributed to μ clusters (below), the average number of usable (i.e., accurate and clean) trials for each condition was: PN = 64.8 (SD = 10.0); TQ = 62.6 (SD = 10.5); TN = 62.3 (SD = 10.0); SQ = 63.1 (SD = 10.4); SN = 61.6 (SD = 9.1).

Figure 3 shows the similar distribution of components that were included based on the a priori criteria in left and right μ clusters for the PWS and control groups. Of the 27 PWS, 23 contributed to left and/or right μ clusters. Specifically, 18 contributed to both clusters while 2 contributed only to the left and 3 only to the right (see Table 1). Of the 27 matched controls, 24 contributed to left and/or right μ clusters. Specifically, 18 contributed to both clusters while 3 contributed only to the left and 3 only to the right.

20/27 PWS contributed to the left μ cluster. Data from the same number of age, gender, and handedness-matched controls were used in group comparisons. The average ages of control and PWS contributors was 28.9 and 27.4 years respectively, which were not significantly different [$t(38)= 0.47$, $p= 0.64$]. The total number of left μ components contributed was 30 for the PWS and 27 for the controls. 21/27 PWS contributed to the right μ cluster. Data from the same number of age, gender, and handedness-matched controls were used in group comparisons. The average ages of control and PWS contributors were 27.52 and 26.38 years respectively, which were not significantly different [$t(40)=0.39$, $p=0.71$]. The total number of right μ components contributed was 30 for the PWS group and 29 for the controls. Table 2

shows average ECD sources and RVs for left and right μ clusters separated by group. As the average ECD sources for the two groups were separated by less than 1 cm, for the purposes of conversion to sLORETA maximum current source densities (CSD), source data from both groups were combined (also shown in Table 2).

3.3. Spectral analyses of μ clusters

Figure 4 shows between-group comparisons of left and right μ spectra across all five conditions. For the left μ, the PWS group displayed reduced spectral power in β frequencies in all discrimination conditions compared to the control group ($p < 0.05$, cluster corrected). For the right μ, the PWS displayed reduced spectral power in β frequencies in all conditions (control and discrimination) compared to the control group ($p < 0.05$, cluster corrected). No spectral differences across conditions were observed for either group. For both left and right μ clusters, the correlations between raw SSI scores and the maximum μ-β spectral power were weak and non-significant ($r = -0.03$ on the left and $r = -0.07$ on the right).

3.4. Time-frequency analyses of μ oscillatory activity

Group differences: Figures 5 and 6 show Van Essen maps (generated using sLORETA) of significant voxels contributing to the left and right μ clusters, respectively. In each figure, these are followed by time-frequency (ERSP) analyses for each condition in both groups across a 7–25 Hz bandwidth, which reflect oscillatory changes in μ frequencies of interest from the prestimulus baseline across trials (before, during and following stimuli). Significant ($p < 0.05$, cluster corrected) between-group differences are also displayed. In the left hemisphere (figure 5) PWS demonstrated increased μ-β ERD in the PN condition. In addition, in the TN and SN conditions, PWS display increased μ-β ERD and reduced μ-α ERS before and during stimulus onset. In the right hemisphere (figure 6), PWS again demonstrated increased μ-β ERD in the PN condition, extending across the entire trial. In the TN condition, PWS exhibit increased μ-β ERD and reduced μ-α ERS before and during stimulus onset. In contrast to the findings in the left μ cluster (above), no group differences were observed in the SN condition.

Within-subject differences: For both groups, all discrimination conditions resulted in widespread time-frequency differences compared to the PN condition. However, since PWS exhibited μ-β ERD in the PN condition, it could not be considered a true control condition. Therefore, PN was considered separately from the discrimination conditions. Post hoc comparisons of the effects of speech versus tone discriminations showed no significant differences for either group. Post hoc comparisons showing the effects of quiet versus noisy discrimination conditions are shown in Figure 7. Controls demonstrated reduced μ-β ERD and greater μ-α ERS in noisy trials before and during stimulus onset in the right hemisphere only. PWS showed bilateral increases μ-α and μ-β ERD in noisy conditions following stimulus offset.

4. Discussion

In this study, ICA on whole-head EEG data from passive listening and auditory discrimination tasks identified left and right sensorimotor μ components from cohorts of

stuttering adults (PWS) and matched controls. In accord with previous studies that used similar inclusion criteria for μ cluster membership (Bowers et al., 2013;Jenson et al., 2014), ~88% of PWS and controls contributed to either left or right μ clusters, while 67% contributed to both. As shown in Figure 3, the distribution of μ dipoles was similar in the left and right hemispheres and between the two groups. Though the average source coordinates identified by the two localization methods (ECD and CSD) varied slightly (by 1.34 cm in the left hemisphere and 0.7 cm on the right), both techniques placed the sources within premotor-motor regions that are accepted generators of μ rhythms (Schnitzler et al., 2000;Pineda, 2005;Hari, 2006;Jenson et al., 2014). The bilateral sensorimotor findings herein are consistent with recent findings in tasks eliciting sensorimotor activity (Yue et al., 2013;Alho et al., 2014;Callan et al., 2014;Cogan et al., 2014). Given the similar numbers of components yielded by each group to left and right μ clusters and their similar localizations, it was possible to test the hypotheses addressing stuttering-related μ spectral and oscillatory differences.

4.1. μ rhythm spectral differences

Supporting the first hypothesis, across all conditions, PWS produced μ spectra with reduced μ-β spectral amplitude (figure 4). Group differences were significant in all 5 conditions for right μ clusters and in all but the PN condition for left μ clusters (figure 4). Overall spectral amplitudes are influenced by oscillatory changes across time. In the current study, this time window included the baseline and the event-related changes in each testing condition. Joos et al. (2014) reported similar group differences in β power averaged across all electrodes for resting state conditions. Taken together, these findings suggest that reduced β spectral amplitude, especially when arising from sensorimotor regions, might be a stable marker of stuttering. Reduced β amplitudes are consistent with a reduced sensorimotor capacity for the generation of forward models (Max et al., 2004a;Daliri and Max, 2015a). As the differences have been observed at resting state (Joos et al., 2014) and now in passive listening and auditory discrimination conditions, data align with a more general sensorimotor deficit, rather than one restricted to speech production (Max et al., 2003;Max and Yudman, 2003;Chang et al., 2009;Daliri et al., 2014).

The possibility of a spectral biomarker for stuttering is not unprecedented. EEG spectral differences have been used to differentiate matched controls from those with pathological conditions like dyslexia (Galin et al., 1992;Papagiannopoulou and Lagopoulos, 2016), insomnia (Buysse et al., 2008), fibromyalgia (Gonzalez-Roldan et al., 2016), epilepsy (Adebimpe et al., 2015), adolescents with sports related concussions (Balkan et al., 2015), and Parkinson's disease (Caviness et al., 2016). In the current study, μ-β amplitudes did not correlate with a behavioral measure of stuttering severity making it unclear how well μ-β amplitude defines the disorder. Replication and extension to populations of children who stutter is necessary before the presence of a spectral biomarker is confirmed. However, the differences in spectral amplitude do predict that in time-frequency analyses, PWS will exhibit greater μ-β ERD (i.e., more desynchronization) than controls across events.

4.2. Between-group time-frequency differences in PN condition

Supporting the prediction above, PWS exhibited significant bilateral μ-β ERD across PN trials (figures 5 and 6). Alternatively, their matched controls demonstrated expectedly low levels of oscillatory activity, similar to control data from previous studies. PN serves as an effective control condition due to its relatively low attentional and motor demands. Therefore, it is interesting to consider how the demands of this task (listening to noise then pressing a button) influences PWS but not their matched controls to induce μ-β ERD.

In regards to the button press, preparatory β ERD typically precedes movements such as a button press by ~1000 ms (Alegre et al., 2003). Therefore, placing a button-press response 1000 ms after the termination of an epoch typically minimizes the effect of pre-movement μ-β ERD within the epoch. Though there is evidence that PWS have general motor planning deficits (Lu et al., 2010a;Daliri et al., 2014;Neef et al., 2015) that may influence motor preparation, it is doubtful that it would influence μ-β ERD up to 5000 ms prior to a simple button press. Alternatively, μ-β ERD (from baseline) began with presentation of noise. Evidence from fMRI suggests that scanner noise (i.e., in excess of 100 dB) can induce motor activity in non stuttering individuals (Cho et al., 1998;Elliott et al., 1999). It seems possible that even lower noise levels might be sufficient to induce motor activity in PWS, especially in light of observed differences in auditory processing that may alter auditory-motor interactions (Hampton and Weber-Fox, 2008;Kikuchi et al., 2011;Mock et al., 2015;Kikuchi et al., 2017). Referencing other developmentally disordered populations (e.g., autism and dyslexia), Halag-Milo et al (2016) address this possibility in a cautionary note following a recent fMRI speech perception study in PWS. Clues to how motor systems in PWS might be impacted by white noise come from studies demonstrating enhancement of fluency under masking (Andrews et al., 1983;Martin et al., 1985;Bloodstein and Ratner, 1995). These effects have been attributed to reducing error detection and repair in auditory regions (Civier et al 2010). A logical consequence also might be heightened motor reactivity to the noise, which appears to be the best explanation for the μ-β ERD observed in PWS in the PN condition and may have influenced discrimination conditions.

4.3. μ-α and μ-β time-frequency differences in discrimination conditions

Speech and tone discrimination conditions were characterized bilaterally by oscillatory changes from baseline in μ-α and μ-β across the time course of events. μ-β oscillatory fluctuations are interpreted to reflect changes in contributions of motor activity across the time course of the discrimination task while μ-α oscillations characterize alterations in sensory feedback from auditory regions. Significant oscillatory differences between- and within-groups were found in the presence of background noise.

4.3.1. Early oscillatory activity—Prior to and during stimulus presentation (segments A and B in figures 4–6), PWS displayed μ-β ERD, which was similar across all conditions (quiet and noise) and predicted by the spectra. μ-β ERD in anticipation of stimuli often is attributed to top-down forward modeling contributing to predictive coding by constraining analysis of forthcoming auditory stimuli (Arnal and Giraud, 2012;Sohoglu et al., 2012). In PWS, the early μ-β ERD observed in the quiet conditions perhaps provides evidence of forward modeling. However, the same pattern was found in the presence of noise and in the

PN condition, making it difficult to ascertain that forward modeling was the only contributor to early μ-β ERD in PWS during discrimination. In contrast, for the control group, noisy discrimination was characterized bilaterally by increased neural synchronization. That is, relative to quiet conditions, controls exhibited reduced μ-β ERD and increased μ-α ERS, consistent with previous work using the same design. However, in the current study, differences only reached significance in the right hemisphere[1]. As α ERS is considered an index of sensory gating, the data suggest that controls exhibited a shift in predictive strategies from forward modeling in quiet conditions to sensory gating of the irrelevant stimuli (i.e., noise) in the noisy conditions.

Group differences may be explained best by the idea that controls dynamically adapt their sensorimotor strategies for discrimination in noise, while strategies of PWS remain relatively static across conditions. The finding of reduced sensory gating (reduced α ERS) in PWS is consistent with MEG findings of reduced P50m suppression responses to tone bursts in the left hemisphere only (Kikuchi et al., 2011). These appear to be the first data to demonstrate functionally that PWS show reduced sensory gating of noise in auditory discrimination. It is noteworthy that in the right hemisphere group differences did not reach significance in the SN condition due to weaker spectral power, perhaps reflecting a reduced role of the right hemisphere in speech processing.

4.3.2. Late oscillatory activity—Following stimulus offset (segment C in figures 4–6), the strongest patterns of μ-α and μ-β ERD were observed bilaterally for both groups in all discrimination conditions. The strong activity suggests that in both groups auditory stimulation updated internal models that were then held in working memory. It also supports notions regarding strong contributions of working memory (possibly via covert replay) to anterior dorsal stream activity observed in auditory discrimination tasks (Burton et al., 2000;Burton et al., 2005). Interestingly, within PWS, post stimulus μ ERD was stronger in noisy conditions (figure 7). The findings suggest that while both groups used updated internal modeling to help keep the stimuli in working memory prior to responding, PWS employed this strategy largely in noisy conditions, possibly to help compensate for sensorimotor deficits early in the trial.

4.5. Speech versus tone discrimination

It is worth noting that oscillatory differences were not observed between speech and tone conditions in either group. Thus, both PWS and controls employed sensorimotor strategies similarly for speech and tone discrimination. This finding is not unusual considering reports of strong overlap between regions involved in speech and non-speech sensorimotor processing when non-speech stimuli are more complex in nature. This suggests that sensorimotor processing helps encode rapid temporal characteristics of acoustic stimuli (Fiez et al., 1996;Zatorre et al., 1999;Poldrack et al., 2001;Joanisse and Gati, 2003;LoCasto et al., 2004;Zaehle et al., 2008;Burton, 2009).

---

[1]Jenson et al., (2014) tested predominantly females, whereas due to the epidemiology of stuttering, controls in the current study were predominantly male. The larger noise-related differences observed in females may be indicative of sex-related sensorimotor processing differences (Thornton et al., in prep).

4.6. Basal ganglia contributions to μ rhythm oscillations

Though μ rhythms typically emanate from sensorimotor sources, there is substantial evidence to indicate that their oscillatory activity can be influenced by contributions from the basal ganglia. First, motor regions are sites of integration for two main basal ganglia based loops in motor control (Band and van Boxtel, 1999;Dillon and Pizzagalli, 2007). Second, reduced β power has been found in response to changes in auditory beats (Fujioka et al., 2010;Fujioka et al., 2015). The findings were thought to reflect the transfer of timing to sensorimotor information through fluctuations in corticobasal-ganglia and thalamocortical circuits, demonstrating how basal ganglia circuits can contribute to forward models by coding changes in predictive timing of auditory information (Arnal 2012; Arnal & Giraud 2012). Stuttering-related differences in β oscillations recently have been found in children (Etchell et al., 2016) and adults (Mersov et al., 2016). Third, selection and inhibition processes modulate and stabilize sensory experience and fluid movements operate through basal ganglia circuits (Buzsaki, 2006;Klimesch et al., 2007;Okun and Lampl, 2008;Jensen and Mazaheri, 2010) and can be measured by changes in α fluctuations across motor regions (Bonstrup et al., 2015). In stuttering, compromises to this mechanism have been implicated in disrupting the inhibition of unwanted syllables during speech production (Civier et al., 2010;Chang and Zhu, 2013;Civier et al., 2013).

4.7. General Discussion

Analyses of μ rhythm spectra followed by task-specific time-frequency decompositions are sensitive to capturing functional neurophysiological differences associated with stuttering. Resting state (Joos et al, 2014) and the current task-related effects converge to suggest that stuttering generally is associated with reduced β spectral amplitudes. Spectral differences are likely to manifest across tasks and be evident in time-frequency analyses. However time-frequency fluctuations represent changes from pre-stimulus baseline, and therefore do not account for any differences in the baseline that are also present in the spectra.

This makes findings from the PN conditions particularly interesting, as they are consistent with time-frequency activity that would be predicted by the spectra and represent noise-induced oscillatory changes from pre-stimulus baseline. If pre-stimulus baseline in the current study is analogous to resting state, the changes in oscillatory activity of PWS during the PN condition (where discrimination is not required) suggest the presence of noise is sufficient to induce motor activity. Thus, scanner noise might have influenced fMRI-based reports of heightened resting state activity across speech motor circuits in PWS (e.g., Xuan 2012). In contrast, using EEG presumably in the absence of background noise, Joos et al (2014) did not identify resting state activity differences between PWS and controls, though they acknowledged their study may have been underpowered for these purposes. Thus, future μ rhythm studies using quiet conditions, devoid of attentional and motor demands, may further understanding of resting state differences versus motor reactivity in PWS. In discrimination conditions, similar patterns of early μ-β ERD observed across conditions was similar to that observed in the PN conditions, made it difficult to determine the contributions of early forward modeling. Taken together spectral differences, along with time-frequency differences in the PN and discrimination conditions, suggest that reduced forward modeling capacities might be related to generally heightened motor reactivity.

Another major finding was that PWS showed significantly reduced sensory gating compared to controls when discriminating in noise. This difference was not observed in the PN condition, during which neither group demonstrated μ-α ERS. This finding provides further evidence of μ-α ERS marking the suppression of irrelevant stimuli for active sensing (Klimesch et al., 2007;Schroeder et al., 2010). As spectral power differences were not observed for μ-α, it is unclear if reduced inhibitory gating in PWS is task specific or a 'signature of stuttering' as suggested by Kikuchi et al. (2011). What does seem apparent is that heightened motor reactivity in combination with reduced inhibitory gating implicate deficiencies in both sensorimotor and basal ganglia function; both of which are thought to contribute to neural dysfunction in stuttering. Because participants were adults, it currently is not possible to distinguish whether the observed differences underlie stuttering or are a consequence of life-long stuttering. Further testing in children is necessary for elaboration.

Discrimination accuracies were generally high and similar between groups. However, PWS displayed poorer discrimination accuracy in tone conditions, though only accuracy in the TQ condition was significantly lower. Analogous findings by Hampton and Weber-Fox (2008) reported differences in discrimination accuracy for non-speech stimuli in children who stutter versus their matched controls. As accuracy levels were similar and only accurate discriminations were considered in the current study, the EEG data are not interpreted in light of the behavioral differences. It is still interesting to note that despite apparent impairments in forward modeling and inhibitory gating, PWS achieved accuracy levels that for the most part, were similar to those of controls. The question of how sensorimotor contributions functionally aid auditory discrimination continue to be debated (Scott et al., 2009;Callan et al., 2010;Hickok et al., 2011;Alho et al., 2014;Carbonell and Lotto, 2014;Skipper, 2014;Skipper et al., 2017). The current findings suggest that, at least in PWS, accurate discrimination was largely accomplished by auditory analysis rather than dorsal stream sensorimotor processing. However, this interpretation is highly speculative without supporting information pertaining to oscillatory activity from auditory regions. A logical next step in this research is to identify and compare activity from auditory components typically characterized by α spectra (Weisz et al., 2011;Weisz and Obleser, 2014; Jenson et al, 2015) in PWS and controls. With this information, it will also be possible to compute effective connectivity, providing temporally precise information regarding the flow of oscillatory information between sensorimotor and auditory regions (Lu et al., 2010b;Friston, 2011)

This study used passive listening and discrimination conditions, with the intention of describing sensorimotor differences associated with stuttering. With the additional consideration that basal ganglia functions also are implicated in the group differences, it is interesting to note some parallels to speech production. First, the relatively static pattern of μ oscillatory activity observed in PWS relative to controls across discrimination events suggests reduced sensorimotor adaptation. In a number of speech production studies, reduced sensorimotor adaptation has been reported in PWS in response to auditory perturbations (Cai et al., 2012;Loucks et al., 2012;Cai et al., 2014;Sengupta et al., 2016). Second, differences were only observed early in the event, before all necessary auditory information had been received to make the discrimination. After hearing the auditory stimuli, both groups responded with similarly strong patterns of μ-α and μ-β ERD,

suggesting that auditory perception had updated models (regardless of their initial integrity) that could be adequately stored in working memory by both groups. In speech production, most stuttering occurs during speech initiation (Brown, 1938;1945;Bloodstein and Grossman, 1981), which has been explained by weak forward models generating weak predictions that result in increased error detection. Similar to what was observed in discrimination tasks in the current study, once auditory feedback is received and internal models are updated, stimulation by auditory targets appears to help normalize sensorimotor processing (Max et al., 2004a;Max et al., 2004b;Civier et al., 2010).

4.7. Caveats

Though all participants produced 'μ-like' components, some (both PWS and controls) did not contribute to μ clusters (Nystrom, 2008;Bowers et al., 2013;Jenson et al., 2014;Cuellar et al., 2016). This is common in oscillatory studies due to inherent inter-individual variability when mapping cognitive functions to cortical topography (Biermann-Ruben et al., 2005;Basile, 2007). The main causes for failure to meet inclusion criteria were 1) the spectra were noisy and did not demonstrate clear α and β peaks, 2) ICA failed to assign what appeared to be a μ component to one of the cortical regions known to generate sensorimotor μ rhythms, or 3) ICA failed to fit a μ component dipole in the sensorimotor region with less than 20% RV. The latter two problems likely stem from the use of standard BESA head models, which reduces source localization accuracy. This continues to highlight the general need for improved spatial resolution in EEG techniques. Of further note, it is unclear how the influence of inaccurate discriminations (though considerably fewer) may affect the neural data.

5. Conclusions

With an eye towards examining oscillatory activity in other components and effective connectivity between components, the current findings demonstrate that μ rhythms provide a rich source of sensorimotor information during auditory perception tasks. When the 'complete' μ rhythm (μ-α and μ-β) is identified and decomposed, cooperation of motor-to-sensory (μ-β) and sensory-to-motor (μ-α) processes are observed across the time course of events. In addition to suggesting heightened motor reactivity in PWS, the current findings indicate that discrimination tasks, especially in noise, are sensitive to forward modeling and auditory-motor feedback compromises that characterize stuttering. Continuing this line of research in both child and adult stuttering populations may lead to clear sensorimotor biomarkers of stuttering that help predict spontaneous recovery, indices of therapy-related cortical changes in those whose stuttering persists, and better separation of causal versus compensatory sensorimotor strategies.

Acknowledgments

References

Adebimpe A, Aarabi A, Bourel-Ponchel E, Mahmoudzadeh M, Wallois F. EEG resting state analysis of cortical sources in patients with benign epilepsy with centrotemporal spikes. Neuroimage Clin. 2015; 9:275–282. [PubMed: 26509114]

Alegre M, Gurtubay IG, Labarga A, Iriarte J, Malanda A, Artieda J. Alpha and beta oscillatory changes during stimulus-induced movement paradigms: effect of stimulus predictability. Neuroreport. 2003; 14:381–385. [PubMed: 12634488]

Alho J, Lin FH, Sato M, Tiitinen H, Sams M, Jaaskelainen IP. Enhanced neural synchrony between left auditory and premotor cortex is associated with successful phonetic categorization. Front Psychol. 2014; 5:394. [PubMed: 24834062]

Alho J, Sato M, Sams M, Schwartz JL, Tiitinen H, Jaaskelainen IP. Enhanced early-latency electromagnetic activity in the left premotor cortex is associated with successful phonetic categorization. Neuroimage. 2012; 60:1937–1946. [PubMed: 22361165]

Alm PA. Stuttering and the basal ganglia circuits: a critical review of possible relations. J Commun Disord. 2004; 37:325–369. [PubMed: 15159193]

Andrews G, Craig A, Feyer AM, Hoddinott S, Howie P, Neilson M. Stuttering: a review of research findings and theories circa 1982. J Speech Hear Disord. 1983; 48:226–246. [PubMed: 6353066]

Arnal LH. Predicting "When" Using the Motor System's Beta-Band Oscillations. Front Hum Neurosci. 2012; 6:225. [PubMed: 22876228]

Arnal LH, Giraud AL. Cortical oscillations and sensory predictions. Trends Cogn Sci. 2012; 16:390–398. [PubMed: 22682813]

Baddeley A. Working memory. Curr Biol. 2010; 20:R136–140. [PubMed: 20178752]

Balkan O, Virji-Babul N, Miyakoshi M, Makeig S, Garudadri H. Source-domain spectral EEG analysis of sports-related concussion via Measure Projection Analysis. Conf Proc IEEE Eng Med Biol Soc. 2015; 2015:4053–4056. [PubMed: 26737184]

Band GP, Van Boxtel GJ. Inhibitory motor control in stop paradigms: review and reinterpretation of neural mechanisms. Acta Psychol (Amst). 1999; 101:179–211. [PubMed: 10344185]

Basile LF. Complex, multifocal, individual-specific attention-related cortical functional circuits. Biol Res. 2007; 40:451–470. [PubMed: 18575678]

Beal DS, Cheyne DO, Gracco VL, Quraan MA, Taylor MJ, De Nil LF. Auditory evoked fields to vocalization during passive listening and active generation in adults who stutter. Neuroimage. 2010; 52:1645–1653. [PubMed: 20452437]

Beal DS, Gracco VL, Brettschneider J, Kroll RM, De Nil LF. A voxel-based morphometry (VBM) analysis of regional grey and white matter volume abnormalities within the speech production network of children who stutter. Cortex. 2013; 49:2151–2161. [PubMed: 23140891]

Beal DS, Gracco VL, Lafaille SJ, De Nil LF. Voxel-based morphometry of auditory and speech-related cortex in stutterers. Neuroreport. 2007; 18:1257–1260. [PubMed: 17632278]

Beal DS, Quraan MA, Cheyne DO, Taylor MJ, Gracco VL, De Nil LF. Speech-induced suppression of evoked auditory fields in children who stutter. Neuroimage. 2011; 54:2994–3003. [PubMed: 21095231]

Bell AJ, Sejnowski TJ. An information-maximization approach to blind separation and blind deconvolution. Neural Comput. 1995; 7:1129–1159. [PubMed: 7584893]

Belyk M, Kraft SJ, Brown S. Stuttering as a trait or state – an ALE meta-analysis of neuroimaging studies. Eur J Neurosci. 2015; 41:275–284. [PubMed: 25350867]

Biermann-Ruben K, Salmelin R, Schnitzler A. Right rolandic activation during speech perception in stutterers: a MEG study. Neuroimage. 2005; 25:793–801. [PubMed: 15808980]

Binder JR, Liebenthal E, Possing ET, Medler DA, Ward BD. Neural correlates of sensory and decision processes in auditory object identification. Nat Neurosci. 2004; 7:295–301. [PubMed: 14966525]

Bloodstein O, Grossman M. Early StutteringsSome Aspects of Their Form and Distribution. Journal of Speech, Language, and Hearing Research. 1981; 24:298–302.

Bloodstein, O., Ratner, N. A handbook on stuttering Singular. San Diego, CA: 1995.

Bonstrup M, Hagemann J, Gerloff C, Sauseng P, Hummel FC. Alpha oscillatory correlates of motor inhibition in the aged brain. Front Aging Neurosci. 2015; 7:193. [PubMed: 26528179]

Bowers A, Saltuklaroglu T, Harkrider A, Cuellar M. Suppression of the micro rhythm during speech and non-speech discrimination revealed by independent component analysis: implications for sensorimotor integration in speech processing. PLoS One. 2013; 8:e72024. [PubMed: 23991030]

Bowers AL, Saltuklaroglu T, Harkrider A, Wilson M, Toner MA. Dynamic modulation of shared sensory and motor cortical rhythms mediates speech and non-speech discrimination performance. Front Psychol. 2014; 5:366. [PubMed: 24847290]

Brinkman L, Stolk A, Dijkerman HC, De Lange FP, Toni I. Distinct roles for alpha- and beta-band oscillations during mental simulation of goal-directed actions. J Neurosci. 2014; 34:14783–14792. [PubMed: 25355230]

Brown S, Ingham RJ, Ingham JC, Laird AR, Fox PT. Stuttered and fluent speech production: an ALE meta-analysis of functional neuroimaging studies. Hum Brain Mapp. 2005; 25:105–117. [PubMed: 15846815]

Brown SF. Stuttering with relation to word accent and word position. The Journal of Abnormal and Social Psychology. 1938; 33:112.

Brown SF. The loci of stutterings in the speech sequence. Journal of Speech Disorders. 1945; 10:181–192.

Brunner C, Delorme A, Makeig S. Eeglab – an Open Source Matlab Toolbox for Electrophysiological Research. Biomed Tech (Berl). 2013

Burton MW. Understanding the role of the prefrontal cortex in phonological processing. Clin Linguist Phon. 2009; 23:180–195. [PubMed: 19283576]

Burton MW, Locasto PC, Krebs-Noble D, Gullapalli RP. A systematic investigation of the functional neuroanatomy of auditory and visual phonological processing. Neuroimage. 2005; 26:647–661. [PubMed: 15955475]

Burton MW, Small SL. Functional neuroanatomy of segmenting speech and nonspeech. Cortex. 2006; 42:644–651. [PubMed: 16881272]

Burton MW, Small SL, Blumstein SE. The role of segmentation in phonological processing: an fMRI investigation. J Cogn Neurosci. 2000; 12:679–690. [PubMed: 10936919]

Buysse DJ, Germain A, Hall ML, Moul DE, Nofzinger EA, Begley A, Ehlers CL, Thompson W, Kupfer DJ. EEG spectral analysis in primary insomnia: NREM period effects and sex differences. Sleep. 2008; 31:1673–1682. [PubMed: 19090323]

Buzsaki, G. Rhythms of the Brain. Oxford University Press; 2006.

Cai S, Beal DS, Ghosh SS, Tiede MK, Guenther FH, Perkell JS. Weak responses to auditory feedback perturbation during articulation in persons who stutter: evidence for abnormal auditory-motor transformation. PLoS One. 2012; 7:e41830. [PubMed: 22911857]

Cai S, Tourville JA, Beal DS, Perkell JS, Guenther FH, Ghosh SS. Diffusion imaging of cerebral white matter in persons who stutter: evidence for network-level anomalies. Front Hum Neurosci. 2014; 8:54. [PubMed: 24611042]

Callan D, Callan A, Gamez M, Sato MA, Kawato M. Premotor cortex mediates perceptual performance. Neuroimage. 2010; 51:844–858. [PubMed: 20184959]

Callan DE, Jones JA, Callan A. Multisensory and modality specific processing of visual speech in different regions of the premotor cortex. Front Psychol. 2014; 5:389. [PubMed: 24860526]

Carbonell KM, Lotto AJ. Speech is not special… again. Front Psychol. 2014; 5:427. [PubMed: 24917830]

Carlqvist H, Nikulin VV, Stromberg JO, Brismar T. Amplitude and phase relationship between alpha and beta oscillations in the human electroencephalogram. Med Biol Eng Comput. 2005; 43:599–607. [PubMed: 16411632]

Caviness JN, Utianski RL, Hentz JG, Beach TG, Dugger BN, Shill HA, Driver-Dunckley ED, Sabbagh MN, Mehta S, Adler CH. Differential spectral quantitative electroencephalography patterns between control and Parkinson's disease cohorts. Eur J Neurol. 2016; 23:387–392. [PubMed: 26518336]

Celsis P, Boulanouar K, Doyon B, Ranjeva JP, Berry I, Nespoulous JL, Chollet F. Differential fMRI responses in the left posterior superior temporal gyrus and left supramarginal gyrus to habituation and change detection in syllables and tones. Neuroimage. 1999; 9:135–144. [PubMed: 9918735]

Chang SE. Research updates in neuroimaging studies of children who stutter. Semin Speech Lang. 2014; 35:67–79. [PubMed: 24875668]

Chang SE, Erickson KI, Ambrose NG, Hasegawa-Johnson MA, Ludlow CL. Brain anatomy differences in childhood stuttering. Neuroimage. 2008; 39:1333–1344. [PubMed: 18023366]

Chang SE, Kenney MK, Loucks TM, Ludlow CL. Brain activation abnormalities during speech and non-speech in stuttering speakers. Neuroimage. 2009; 46:201–212. [PubMed: 19401143]

Chang SE, Zhu DC. Neural network connectivity differences in children who stutter. Brain. 2013; 136:3709–3726. [PubMed: 24131593]

Cheyne D, Gaetz W, Garnero L, Lachaux JP, Ducorps A, Schwartz D, Varela FJ. Neuromagnetic imaging of cortical oscillations accompanying tactile stimulation. Brain Res Cogn Brain Res. 2003; 17:599–611. [PubMed: 14561448]

Cheyne DO. MEG studies of sensorimotor rhythms: a review. Exp Neurol. 2013; 245:27–39. [PubMed: 22981841]

Cho ZH, Chung SC, Lim DW, Wong EK. Effects of the acoustic noise of the gradient systems on fMRI: a study on auditory, motor, and visual cortices. Magn Reson Med. 1998; 39:331–335. [PubMed: 9469720]

Cieslak M, Ingham RJ, Ingham JC, Grafton ST. Anomalous white matter morphology in adults who stutter. J Speech Lang Hear Res. 2015; 58:268–277. [PubMed: 25635376]

Civier O, Bullock D, Max L, Guenther FH. Computational modeling of stuttering caused by impairments in a basal ganglia thalamo-cortical circuit involved in syllable selection and initiation. Brain Lang. 2013; 126:263–278. [PubMed: 23872286]

Civier O, Tasko SM, Guenther FH. Overreliance on auditory feedback may lead to sound/syllable repetitions: simulations of stuttering and fluency-inducing conditions with a neural model of speech production. Journal of fluency disorders. 2010; 35:246–279. [PubMed: 20831971]

Cogan GB, Thesen T, Carlson C, Doyle W, Devinsky O, Pesaran B. Sensory-motor transformations for speech occur bilaterally. Nature. 2014; 507:94–98. [PubMed: 24429520]

Connally EL, Ward D, Howell P, Watkins KE. Disrupted white matter in language and motor tracts in developmental stuttering. Brain Lang. 2014; 131:25–35. [PubMed: 23819900]

Corbera S, Corral MJ, Escera C, Idiazabal MA. Abnormal speech sound representation in persistent developmental stuttering. Neurology. 2005; 65:1246–1252. [PubMed: 16247052]

Crawcour S, Bowers A, Harkrider A, Saltuklaroglu T. Mu wave suppression during the perception of meaningless syllables: EEG evidence of motor recruitment. Neuropsychologia. 2009; 47:2558–2563. [PubMed: 19442676]

Cuellar M, Bowers A, Harkrider AW, Wilson M, Saltuklaroglu T. Mu suppression as an index of sensorimotor contributions to speech processing: evidence from continuous EEG signals. Int J Psychophysiol. 2012; 85:242–248. [PubMed: 22522370]

Cuellar M, Harkrider AW, Jenson D, Thornton D, Bowers A, Saltuklaroglu T. Time-frequency analysis of the EEG mu rhythm as a measure of sensorimotor integration in the later stages of swallowing. Clin Neurophysiol. 2016; 127:2625–2635. [PubMed: 27291882]

Daliri A, Max L. Electrophysiological evidence for a general auditory prediction deficit in adults who stutter. Brain Lang. 2015a; 150:37–44. [PubMed: 26335995]

Daliri A, Max L. Modulation of auditory processing during speech movement planning is limited in adults who stutter. Brain Lang. 2015b; 143:59–68. [PubMed: 25796060]

Daliri A, Prokopenko RA, Flanagan JR, Max L. Control and prediction components of movement planning in stuttering vs. nonstuttering adults. Journal of speech, language, and hearing research: JSLHR. 2014; 57:2131–2141.

De Lange FP, Jensen O, Bauer M, Toni I. Interactions between posterior gamma and frontal alpha/beta oscillations during imagined actions. Front Hum Neurosci. 2008; 2:7. [PubMed: 18958208]

Delorme A, Palmer J, Onton J, Oostenveld R, Makeig S. Independent EEG sources are dipolar. PLoS One. 2012; 7:e30135. [PubMed: 22355308]

Dillon DG, Pizzagalli DA. Inhibition of Action, Thought, and Emotion: A Selective Neurobiological Review. Appl Prev Psychol. 2007; 12:99–114. [PubMed: 19050749]

Donner TH, Siegel M, Fries P, Engel AK. Buildup of choice-predictive activity in human motor cortex during perceptual decision making. Curr Biol. 2009; 19:1581–1585. [PubMed: 19747828]

Elliott MR, Bowtell RW, Morris PG. The effect of scanner sound in visual, motor, and auditory functional MRI. Magn Reson Med. 1999; 41:1230–1235. [PubMed: 10371456]

Engel AK, Fries P. Beta-band oscillations–signalling the status quo? Curr Opin Neurobiol. 2010; 20:156–165. [PubMed: 20359884]

Etchell AC, Johnson BW, Sowman PF. Beta oscillations, timing, and stuttering. Frontiers in Human Neuroscience. 2014; 8:1036. [PubMed: 25601832]

Etchell AC, Ryan M, Martin E, Johnson BW, Sowman PF. Abnormal time course of low beta modulation in non-fluent preschool children: A magnetoencephalographic study of rhythm tracking. Neuroimage. 2016; 125:953–963. [PubMed: 26545455]

Fiez JA, Raichle ME, Balota DA, Tallal P, Petersen SE. PET activation of posterior temporal regions during auditory word presentation and verb generation. Cereb Cortex. 1996; 6:1–10. [PubMed: 8670633]

Frenkel-Toledo S, Bentin S, Perry A, Liebermann DG, Soroker N. Mirror-neuron system recruitment by action observation: effects of focal brain damage on mu suppression. Neuroimage. 2014; 87:127–137. [PubMed: 24140938]

Friston KJ. Functional and effective connectivity: a review. Brain Connect. 2011; 1:13–36. [PubMed: 22432952]

Fujioka T, Ross B, Trainor LJ. Beta-Band Oscillations Represent Auditory Beat and Its Metrical Hierarchy in Perception and Imagery. J Neurosci. 2015; 35:15187–15198. [PubMed: 26558788]

Fujioka T, Zendel BR, Ross B. Endogenous neuromagnetic activity for mental hierarchy of timing. J Neurosci. 2010; 30:3458–3466. [PubMed: 20203205]

Gaetz W, Cheyne D. Localization of sensorimotor cortical rhythms induced by tactile stimulation using spatially filtered MEG. Neuroimage. 2006; 30:899–908. [PubMed: 16326116]

Galin D, Raz J, Fein G, Johnstone J, Herron J, Yingling C. EEG spectra in dyslexic and normal readers during oral and silent reading. Electroencephalogr Clin Neurophysiol. 1992; 82:87–101. [PubMed: 1370788]

Gao Z, Bentin S, Shen M. Rehearsing biological motion in working memory: an EEG study. J Cogn Neurosci. 2015; 27:198–209. [PubMed: 25061930]

Gonzalez-Roldan AM, Cifre I, Sitges C, Montoya P. Altered Dynamic of EEG Oscillations in Fibromyalgia Patients at Rest. Pain Med. 2016

Grabski K, Tremblay P, Gracco VL, Girin L, Sato M. A mediating role of the auditory dorsal pathway in selective adaptation to speech: a state-dependent transcranial magnetic stimulation study. Brain Res. 2013; 1515:55–65. [PubMed: 23542585]

Graimann B, Pfurtscheller G. Quantification and visualization of event-related changes in oscillatory brain activity in the time-frequency domain. Prog Brain Res. 2006; 159:79–97. [PubMed: 17071225]

Halag-Milo T, Stoppelman N, Kronfeld-Duenias V, Civier O, Amir O, Ezrati-Vinacour R, Ben-Shachar M. Beyond production: Brain responses during speech perception in adults who stutter. Neuroimage Clin. 2016; 11:328–338. [PubMed: 27298762]

Hampton A, Weber-Fox C. Non-linguistic auditory processing in stuttering: evidence from behavior and event-related brain potentials. J Fluency Disord. 2008; 33:253–273. [PubMed: 19328979]

Hari R. Action-perception connection and the cortical mu rhythm. Prog Brain Res. 2006; 159:253–260. [PubMed: 17071236]

Hauswald A, Weisz N, Bentin S, Kissler J. MEG premotor abnormalities in children with Asperger's syndrome: determinants of social behavior? Dev Cogn Neurosci. 2013; 5:95–105. [PubMed: 23500669]

Hickok G, Buchsbaum B, Humphries C, Muftuler T. Auditory-motor interaction revealed by fMRI: speech, music, and working memory in area Spt. J Cogn Neurosci. 2003; 15:673–682. [PubMed: 12965041]

Hickok G, Houde J, Rong F. Sensorimotor integration in speech processing: computational basis and neural organization. Neuron. 2011; 69:407–422. [PubMed: 21315253]

Hickok G, Poeppel D. Dorsal and ventral streams: a framework for understanding aspects of the functional anatomy of language. Cognition. 2004; 92:67–99. [PubMed: 15037127]

Houde JF, Chang EF. The cortical computations underlying feedback control in vocal production. Curr Opin Neurobiol. 2015; 33:174–181. [PubMed: 25989242]

Houde JF, Nagarajan SS. Speech production as state feedback control. Front Hum Neurosci. 2011; 5:82. [PubMed: 22046152]

Howell P. The effects of gated speech on the fluency of speakers who stutter. Folia Phoniatr Logop. 2007; 59:250–255. [PubMed: 17726328]

Jansson-Verkasalo E, Eggers K, Jarvenpaa A, Suominen K, Van Den Bergh B, De Nil L, Kujala T. Atypical central auditory speech-sound discrimination in children who stutter as indexed by the mismatch negativity. J Fluency Disord. 2014; 41:1–11. [PubMed: 25066139]

Jasper HH. The ten twenty electrode system of the international federation. Electroencephalography and Clinical Neurophysiology. 1958; 10:371–375.

Jensen O, Mazaheri A. Shaping functional architecture by oscillatory alpha activity: gating by inhibition. Front Hum Neurosci. 2010; 4:186. [PubMed: 21119777]

Jenson D, Bowers AL, Harkrider AW, Thornton D, Cuellar M, Saltuklaroglu T. Temporal dynamics of sensorimotor integration in speech perception and production: independent component analysis of EEG data. Front Psychol. 2014; 5:656. [PubMed: 25071633]

Jenson DE, Harkrider AW, Thornton D, Bowers AL, Saltuklaroglu T. Auditory Cortical Deactivation during Speech Production and following Speech Perception: An EEG investigation of the temporal dynamics of the auditory alpha rhythm. Frontiers in Human Neuroscience. 2015; 9:534. [PubMed: 26500519]

Joanisse MF, Gati JS. Overlapping neural regions for processing rapid temporal cues in speech and nonspeech signals. Neuroimage. 2003; 19:64–79. [PubMed: 12781727]

Joos K, De Ridder D, Boey RA, Vanneste S. Functional connectivity changes in adults with developmental stuttering: a preliminary study using quantitative electro-encephalography. Front Hum Neurosci. 2014; 8:783. [PubMed: 25352797]

Jurkiewicz MT, Gaetz WC, Bostan AC, Cheyne D. Post-movement beta rebound is generated in motor cortex: evidence from neuromagnetic recordings. Neuroimage. 2006; 32:1281–1289. [PubMed: 16863693]

Kell CA, Neumann K, Von Kriegstein K, Posenenske C, Von Gudenberg AW, Euler H, Giraud AL. How the brain repairs stuttering. Brain. 2009; 132:2747–2760. [PubMed: 19710179]

Keough D, Jones JA. Contextual cuing contributes to the independent modification of multiple internal models for vocal control. J Neurophysiol. 2011; 105:2448–2456. [PubMed: 21346208]

Kikuchi Y, Ogata K, Umesaki T, Yoshiura T, Kenjo M, Hirano Y, Okamoto T, Komune S, Tobimatsu S. Spatiotemporal signatures of an abnormal auditory system in stuttering. Neuroimage. 2011; 55:891–899. [PubMed: 21232617]

Kikuchi Y, Okamoto T, Ogata K, Hagiwara K, Umezaki T, Kenjo M, Nakagawa T, Tobimatsu S. Abnormal auditory synchronization in stuttering: A magnetoencephalographic study. Hear Res. 2017; 344:82–89. [PubMed: 27825021]

Klimesch W. alpha-band oscillations, attention, and controlled access to stored information. Trends Cogn Sci. 2012; 16:606–617. [PubMed: 23141428]

Klimesch W, Sauseng P, Hanslmayr S. EEG alpha oscillations: the inhibition-timing hypothesis. Brain Res Rev. 2007; 53:63–88. [PubMed: 16887192]

Kodama T, Nakano H, Ohsugi H, Murata S. Effects of vibratory stimulation-induced kinesthetic illusions on the neural activities of patients with stroke. J Phys Ther Sci. 2016; 28:419–425. [PubMed: 27065525]

Lee TW, Girolami M, Sejnowski TJ. Independent component analysis using an extended infomax algorithm for mixed subgaussian and supergaussian sources. Neural Comput. 1999; 11:417–441. [PubMed: 9950738]

Lewis AG, Schoffelen JM, Schriefers H, Bastiaansen M. A Predictive Coding Perspective on Beta Oscillations during Sentence-Level Language Comprehension. Front Hum Neurosci. 2016; 10:85. [PubMed: 26973500]

Liebenthal E, Sabri M, Beardsley SA, Mangalathu-Arumana J, Desai A. Neural dynamics of phonological processing in the dorsal auditory stream. J Neurosci. 2013; 33:15414–15424. [PubMed: 24068810]

Liotti M, Ingham JC, Takai O, Paskos DK, Perez R, Ingham RJ. Spatiotemporal dynamics of speech sound perception in chronic developmental stuttering. Brain Lang. 2010; 115:141–147. [PubMed: 20810160]

Locasto PC, Krebs-Noble D, Gullapalli RP, Burton MW. An fMRI investigation of speech and tone segmentation. J Cogn Neurosci. 2004; 16:1612–1624. [PubMed: 15601523]

Loucks T, Chon H, Han W. Audiovocal integration in adults who stutter. Int J Lang Commun Disord. 2012; 47:451–456. [PubMed: 22788230]

Loucks T, Kraft SJ, Choo AL, Sharma H, Ambrose NG. Functional brain activation differences in stuttering identified with a rapid fMRI sequence. Journal of fluency disorders. 2011; 36:302–307. [PubMed: 22133409]

Loucks TM, De Nil LF. Anomalous sensorimotor integration in adults who stutter: a tendon vibration study. Neurosci Lett. 2006; 402:195–200. [PubMed: 16698179]

Loucks TM, De Nil LF, Sasisekaran J. Jaw-phonatory coordination in chronic developmental stuttering. J Commun Disord. 2007; 40:257–272. [PubMed: 16889790]

Lu C, Chen C, Ning N, Ding G, Guo T, Peng D, Yang Y, Li K, Lin C. The neural substrates for atypical planning and execution of word production in stuttering. Exp Neurol. 2010a; 221:146–156. [PubMed: 19879262]

Lu C, Long Y, Zheng L, Shi G, Liu L, Ding G, Howell P. Relationship between Speech Production and Perception in People Who Stutter. Front Hum Neurosci. 2016; 10:224. [PubMed: 27242487]

Lu C, Peng D, Chen C, Ning N, Ding G, Li K, Yang Y, Lin C. Altered effective connectivity and anomalous anatomy in the basal ganglia-thalamocortical circuit of stuttering speakers. Cortex. 2010b; 46:49–67. [PubMed: 19375076]

Makeig S, Bell AJ, Jung TP, Sejnowski TJ. Independent component analysis of electroencephalographic data. Advances in neural information processing systems. 1996:145–151.

Makeig S, Debener S, Onton J, Delorme A. Mining event-related brain dynamics. Trends in cognitive sciences. 2004; 8:204–210. [PubMed: 15120678]

Makeig S, Jung TP, Bell AJ, Ghahremani D, Sejnowski TJ. Blind separation of auditory event-related brain responses into independent components. Proc Natl Acad Sci U S A. 1997; 94:10979–10984. [PubMed: 9380745]

Maris E, Oostenveld R. Nonparametric statistical testing of EEG- and MEG-data. J Neurosci Methods. 2007; 164:177–190. [PubMed: 17517438]

Martin RR, Johnson LJ, Siegel GM, Haroldson SK. Auditory stimulation, rhythm, and stuttering. J Speech Hear Res. 1985; 28:487–495. [PubMed: 4087883]

Mathias B, Palmer C, Perrin F, Tillmann B. Sensorimotor Learning Enhances Expectations During Auditory Perception. Cereb Cortex. 2015; 25:2238–2254. [PubMed: 24621528]

Max L, Caruso AJ, Gracco VL. Kinematic analyses of speech, orofacial nonspeech, and finger movements in stuttering and nonstuttering adults. J Speech Lang Hear Res. 2003; 46:215–232. [PubMed: 12647900]

Max L, Guenther FH, Gracco VL, Ghosh SS, Wallace ME. Unstable or insufficiently activated internal models and feedback-biased motor control as sources of dysfluency: A theoretical model of stuttering. Contemporary issues in communication science and disorders. 2004a; 31:105–122.

Max L, Maassen B, Kent R, Peters H, Van Lieshout P, Hulstijn W. Stuttering and internal models for sensorimotor control: A theoretical perspective to generate testable hypotheses. Speech motor control in normal and disordered speech. 2004b:357–387.

Max L, Yudman EA. Accuracy and variability of isochronous rhythmic timing across motor systems in stuttering versus nonstuttering individuals. J Speech Lang Hear Res. 2003; 46:146–163. [PubMed: 12647895]

Mersov AM, Jobst C, Cheyne DO, De Nil L. Sensorimotor Oscillations Prior to Speech Onset Reflect Altered Motor Networks in Adults Who Stutter. Front Hum Neurosci. 2016; 10:443. [PubMed: 27642279]

Mock JR, Foundas AL, Golob EJ. Speech preparation in adults with persistent developmental stuttering. Brain Lang. 2015; 149:97–105. [PubMed: 26197258]

Neef NE, Anwander A, Friederici AD. The Neurobiological Grounding of Persistent Stuttering: from Structure to Function. Curr Neurol Neurosci Rep. 2015; 15:63. [PubMed: 26228377]

Neef NE, Sommer M, Neef A, Paulus W, Von Gudenberg AW, Jung K, Wustenberg T. Reduced speech perceptual acuity for stop consonants in individuals who stutter. J Speech Lang Hear Res. 2012; 55:276–289. [PubMed: 22337496]

Neilson MD, Neilson PD. Speech motor control and stuttering: A computational model of adaptive sensory-motor processing. Speech Communication. 1987; 6:325–333.

Niedermeyer, E., Da Silva, FL. Electroencephalography: basic principles, clinical applications, and related fields. Lippincott Williams & Wilkins; 2005.

Nystrom P. The infant mirror neuron system studied with high density EEG. Soc Neurosci. 2008; 3:334–347. [PubMed: 18979389]

Okun M, Lampl I. Instantaneous correlation of excitation and inhibition during ongoing and sensory-evoked activities. Nat Neurosci. 2008; 11:535–537. [PubMed: 18376400]

Oldfield RC. The assessment and analysis of handedness: the Edinburgh inventory. Neuropsychologia. 1971; 9:97–113. [PubMed: 5146491]

Oostenveld R, Oostendorp TF. Validating the boundary element method for forward and inverse EEG computations in the presence of a hole in the skull. Hum Brain Mapp. 2002; 17:179–192. [PubMed: 12391571]

Osnes B, Hugdahl K, Specht K. Effective connectivity analysis demonstrates involvement of premotor cortex during speech perception. Neuroimage. 2011; 54:2437–2445. [PubMed: 20932914]

Pandey AK, Kamarajan C, Manz N, Chorlian DB, Stimus A, Porjesz B. Delta, theta, and alpha event-related oscillations in alcoholics during Go/NoGo task: Neurocognitive deficits in execution, inhibition, and attention processing. Prog Neuropsychopharmacol Biol Psychiatry. 2016; 65:158–171. [PubMed: 26456730]

Papagiannopoulou EA, Lagopoulos J. Resting State EEG Hemispheric Power Asymmetry in Children with Dyslexia. Front Pediatr. 2016; 4:11. [PubMed: 26942169]

Pascual-Marqui RD. Standardized low-resolution brain electromagnetic tomography (sLORETA): technical details. Methods Find Exp Clin Pharmacol. 2002; 24(Suppl D):5–12. [PubMed: 12575463]

Pecenka N, Engel A, Keller PE. Neural correlates of auditory temporal predictions during sensorimotor synchronization. Front Hum Neurosci. 2013; 7:380. [PubMed: 23970857]

Peled-Avron L, Levy-Gigi E, Richter-Levin G, Korem N, Shamay-Tsoory SG. The role of empathy in the neural responses to observed human social touch. Cogn Affect Behav Neurosci. 2016

Pfurtscheller G. Central beta rhythm during sensorimotor activities in man. Electroencephalogr Clin Neurophysiol. 1981; 51:253–264. [PubMed: 6163614]

Pineda JA. The functional significance of mu rhythms: translating "seeing" and "hearing" into "doing". Brain Res Brain Res Rev. 2005; 50:57–68. [PubMed: 15925412]

Pineda JA, Grichanik M, Williams V, Trieu M, Chang H, Keysers C. EEG sensorimotor correlates of translating sounds into actions. Front Neurosci. 2013; 7:203. [PubMed: 24376395]

Poldrack RA, Temple E, Protopapas A, Nagarajan S, Tallal P, Merzenich M, Gabrieli JD. Relations between the neural bases of dynamic auditory processing and phonological processing: evidence from fMRI. J Cogn Neurosci. 2001; 13:687–697. [PubMed: 11506664]

Pugh KR, Offywitz BA, Shaywitz SE, Fulbright RK, Byrd D, Skudlarski P, Shankweiler DP, Katz L, Constable RT, Fletcher J, Lacadie C, Marchione K, Gore JC. Auditory selective attention: an fMRI investigation. Neuroimage. 1996; 4:159–173. [PubMed: 9345506]

Riley, G. Stuttering severity instrument. Pro-ed; 2009.

Robb MP, Lynn WL, O'beirne GA. An exploration of dichotic listening among adults who stutter. Clin Linguist Phon. 2013; 27:681–693. [PubMed: 23806131]

Ruther NN, Brown EC, Klepp A, Bellebaum C. Observed manipulation of novel tools leads to mu rhythm suppression over sensory-motor cortices. Behav Brain Res. 2014; 261:328–335. [PubMed: 24393742]

Sato M, Tremblay P, Gracco VL. A mediating role of the premotor cortex in phoneme segmentation. Brain Lang. 2009; 111:1–7. [PubMed: 19362734]

Schnitzler A, Gross J, Timmermann L. Synchronised oscillations of the human sensorimotor cortex. Acta Neurobiol Exp (Wars). 2000; 60:271–287. [PubMed: 10909184]

Schroeder CE, Wilson DA, Radman T, Scharfman H, Lakatos P. Dynamics of Active Sensing and Perceptual Selection. Current opinion in neurobiology. 2010; 20:172–176. [PubMed: 20307966]

Scott SK, Mcgettigan C, Eisner F. A little more conversation, a little less action–candidate roles for the motor cortex in speech perception. Nat Rev Neurosci. 2009; 10:295–302. [PubMed: 19277052]

Sebastiani V, De Pasquale F, Costantini M, Mantini D, Pizzella V, Romani GL, Della Penna S. Being an agent or an observer: different spectral dynamics revealed by MEG. Neuroimage. 2014; 102(Pt 2):717–728. [PubMed: 25175536]

Seeber M, Scherer R, Wagner J, Solis-Escalante T, Muller-Putz GR. EEG beta suppression and low gamma modulation are different elements of human upright walking. Front Hum Neurosci. 2014; 8:485. [PubMed: 25071515]

Sengupta R, Shah S, Gore K, Loucks T, Nasir SM. Anomaly in neural phase coherence accompanies reduced sensorimotor integration in adults who stutter. Neuropsychologia. 2016; 93:242–250. [PubMed: 27833009]

Shadmehr R, Smith MA, Krakauer JW. Error correction, sensory prediction, and adaptation in motor control. Annu Rev Neurosci. 2010; 33:89–108. [PubMed: 20367317]

Skipper JI. Echoes of the spoken past: how auditory cortex hears context during speech perception. Philos Trans R Soc Lond B Biol Sci. 2014; 369 20130297.

Skipper JI, Devlin JT, Lametti DR. The hearing ear is always found close to the speaking tongue: Review of the role of the motor system in speech perception. Brain Lang. 2017; 164:77–105. [PubMed: 27821280]

Sohoglu E, Peelle JE, Carlyon RP, Davis MH. Predictive top-down integration of prior knowledge during speech perception. J Neurosci. 2012; 32:8443–8453. [PubMed: 22723684]

Sommer M, Koch MA, Paulus W, Weiller C, Buchel C. Disconnection of speech-relevant brain areas in persistent developmental stuttering. Lancet. 2002; 360:380–383. [PubMed: 12241779]

Tamura T, Gunji A, Takeichi H, Shigemasu H, Inagaki M, Kaga M, Kitazaki M. Audio-vocal monitoring system revealed by mu-rhythm activity. Front Psychol. 2012; 3:225. [PubMed: 22783219]

Tian X, Poeppel D. Mental imagery of speech: linking motor and perceptual systems through internal simulation and estimation. Front Hum Neurosci. 2012; 6:314. [PubMed: 23226121]

Toro C, Deuschl G, Thatcher R, Sato S, Kufta C, Hallett M. Event-related desynchronization and movement-related cortical potentials on the ECoG and EEG. Electroencephalogr Clin Neurophysiol. 1994; 93:380–389. [PubMed: 7525246]

Towle VL, Bolanos J, Suarez D, Tan K, Grzeszczuk R, Levin DN, Cakmur R, Frank SA, Spire JP. The spatial location of EEG electrodes: locating the best-fitting sphere relative to cortical anatomy. Electroencephalography and clinical neurophysiology. 1993; 86:1–6. [PubMed: 7678386]

Toyomura A, Fujii T, Kuriki S. Effect of external auditory pacing on the neural activity of stuttering speakers. Neuroimage. 2011; 57:1507–1516. [PubMed: 21624474]

Tsuchida K, Ueno K, Shimada S. Motor area activity for action-related and nonaction-related sounds in a three-dimensional sound field reproduction system. Neuroreport. 2015; 26:291–295. [PubMed: 25714418]

Urgen BA, Plank M, Ishiguro H, Poizner H, Saygin AP. EEG theta and Mu oscillations during perception of human and robot actions. Front Neurorobot. 2013; 7:19. [PubMed: 24348375]

Venezia JH, Saberi K, Chubb C, Hickok G. Response Bias Modulates the Speech Motor System during Syllable Discrimination. Front Psychol. 2012; 3:157. [PubMed: 22723787]

Watkins KE, Smith SM, Davis S, Howell P. Structural and functional abnormalities of the motor system in developmental stuttering. Brain. 2008; 131:50–59. [PubMed: 17928317]

Weber-Fox C, Spencer RM, Spruill JE 3rd, Smith A. Phonologic processing in adults who stutter: electrophysiological and behavioral evidence. J Speech Lang Hear Res. 2004; 47:1244–1258. [PubMed: 15842008]

Wymbs NF, Ingham RJ, Ingham JC, Paolini KE, Grafton ST. Individual differences in neural regions functionally related to real and imagined stuttering. Brain Lang. 2013; 124:153–164. [PubMed: 23333668]

Yue Q, Zhang L, Xu G, Shu H, Li P. Task-modulated activation and functional connectivity of the temporal and frontal areas during speech comprehension. Neuroscience. 2013; 237:87–95. [PubMed: 23357111]

Zaehle T, Geiser E, Alter K, Jancke L, Meyer M. Segmental processing in the human auditory dorsal stream. Brain Res. 2008; 1220:179–190. [PubMed: 18096139]

Zatorre RJ, Mondor TA, Evans AC. Auditory attention to space and frequency activates similar cerebral systems. Neuroimage. 1999; 10:544–554. [PubMed: 10547331]

Highlights

- Mu *(μ)* rhythms identified in stuttering and matched control groups in auditory discrimination

- Mu *(μ)* rhythm spectra show reduced forward modeling capacity in stuttering group

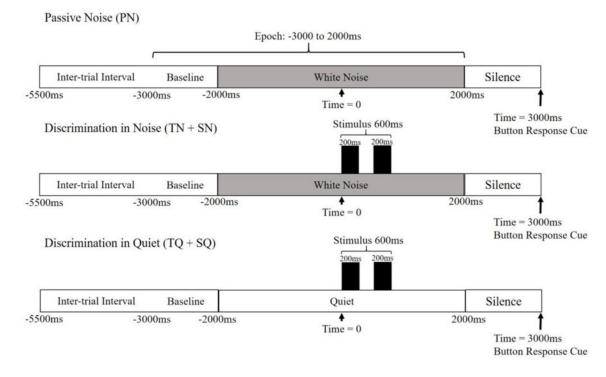- Time-frequency analyses show group differences in predictive coding strategies

Figure 1.
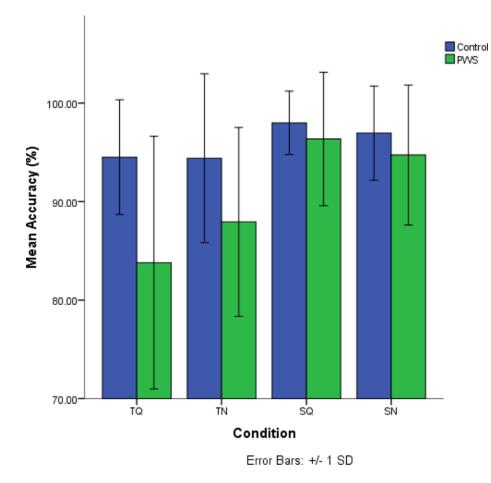Epoch Timeline. 5000 ms epoch time lines for all conditions. In discrimination conditions, stimuli onset is at t=0.

Figure 2.
Behavioral Data. Discrimination accuracy for Controls and PWS who contributed to either left or right μ cluster.
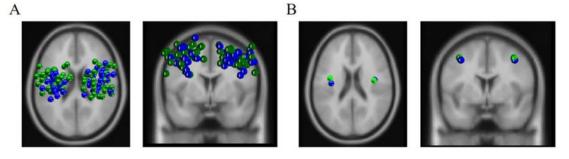
Figure 3.
Equivalent Current Dipole Distributions. A) Transverse and coronal views of all left and right μ dipole sources from both groups. B) Transverse and coronal views of average left and right μ dipoles sources. Green dipoles are from PWS and blue dipoles are from controls.
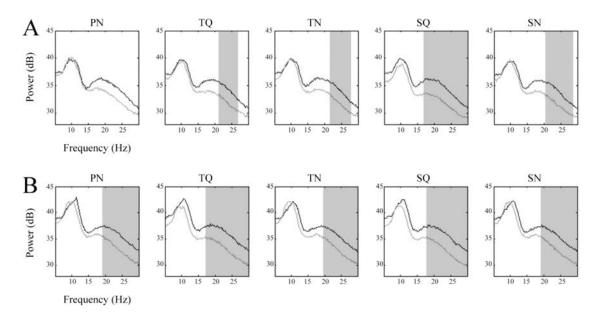
Figure 4.

μ Spectral Comparisons. A) left and B) right average μ spectra from all conditions. Light traces are from PWS and dark traces are from controls. Shaded areas indicate frequencies where significantly different ($p < 0.05$) spectral amplitudes were found (after cluster-based corrections for multiple comparisons).
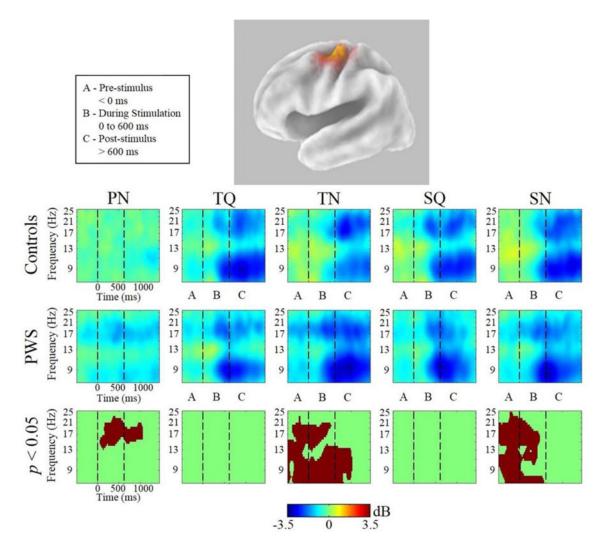
Figure 5.
Left μ Time-Frequency Analyses. sLORETA source solution for combined cluster of all left μ components followed by time-frequency analyses of left μ oscillatory activity from all conditions from PWS and control subjects. Stimulus onset is at t=0. Warmer colors indicate event-related synchronization and cooler colors indicate event-related desynchronization. The lower panels indicate the time-frequency voxels that were significantly different ($p < 0.05$) between the groups (after cluster-based corrections for multiple comparisons).

Figure 6.
Right μ Time-Frequency Analyses. sLORETA source solution for combined cluster of all right μ components followed by time-frequency analyses of right μ oscillatory activity from all conditions from PWS and control subjects. Stimulus onset is at t=0. Warmer colors indicate event-related synchronization and cooler colors indicate event-related desynchronization. The lower panels indicate the time-frequency voxels that were significantly different ($p < 0.05$) between the groups (after cluster-based corrections for multiple comparisons).
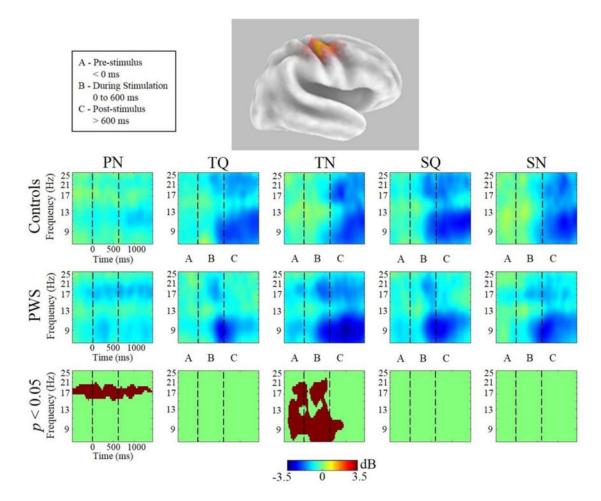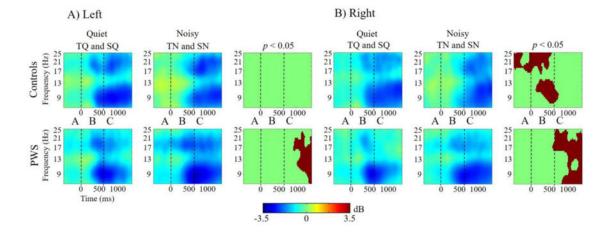
Figure 7.
Within-subject Time-Frequency Contrasts. Differences in quiet versus noisy conditions in A) left μ and B) right μ clusters. Stimulus onset is at t=0. Warmer colors indicate event-related synchronization and cooler colors indicate event-related desynchronization. Panels on the right indicate the time-frequency voxels that were significantly different ($p < 0.05$) between stimulus types for each group (after cluster-based corrections for multiple comparisons).

Table 1

Age, sex, handedness, stuttering severity (according to SSI-4; Riley 2009) and μ cluster contribution of stuttering participants. Severities ranged from very mild (v. mild) to very severe (v. severe). The last column applies to the results of the study, showing how each participant contributed to left and right clusters. L indicates participant contributed to left μ cluster and R indicates participant contributed to right μ cluster.

Stuttering Subject	Age	Sex	Handedness	Severity	μ Cluster Contribution
1	22	M	R	V. Mild	R
2	20	F	R	V. severe	–
3	40	M	R	V. Mild	LR
4	17	F	R	Mild	LR
5	46	M	R	V. Mild	L
6	52	M	R	V. Severe	LR
7	22	M	R	V. Mild	LR
8	32	M	R	V. Mild	LR
9	37	M	R	Mild	R
10	28	F	R	V. Mild	LR
11	36	M	L	Mild	LR
12	26	M	R	Mild	LR
13	26	F	R	V. Severe	L
14	18	F	R	V. Mild	LR
15	18	M	R	V. Mild	LR
16	18	F	R	V. Mild	–
17	22	M	R	V. Mild	LR
18	18	M	R	V. Mild	LR
19	32	M	R	Moderate	LR
20	18	M	R	Moderate	–
21	19	M	L	Mild	LR
22	41	M	R	Moderate	–
23	23	F	R	V. Mild	R
24	23	M	L	Mild	LR
25	18	F	R	V. Mild	LR
26	33	M	R	V. Mild	LR

Stuttering Subject	Age	Sex	Handedness	Severity	μ Cluster Contribution
27	18	F	R	V. Mild	R

Table 2

Source information for left and right μ clusters.

Source Information	Left μ	Right μ
Separated by group		
Controls: Mean ECD source	−35, −12, 43 (BA 6)	39, −6, 43 (BA 6)
Mean Residual variance (RV)	8.16%	6.64%
PWS: Mean ECD source	−37, −4, 45 (BA 6)	38, −7, 45 (BA 6)
Mean Residual variance (RV)	9.64%	8.27%
Distance between sources	0.84 cm	0.25 cm
Control and PWS groups combined		
Mean ECD source	37, −8, 44 (BA 6)	38, −7,44 (BA 6)
Maximum CSD source	40, −15, 55 (BA 4)	40, −10, 50 (BA 6)
Distance between sources	1.34 cm	0.70 cm